Figure 3. High levels of extracellular L-Cystine promoted the L-Cystine-L-Glutamate antiport via xCT and decreased the intracellular GSH/GSSG ratio in monocyte under the amino acid environment of patients with advanced cirrhosis. A, THP-1, Jurkat and Molt-4 cultured under CCM were harvested and labeled with antibodies (CD98, xCT or the relevant isotype controls). Using flow cytometry, surface marker expressions were analyzed. The figure expresses the mean fluorescence intensity. Data shown are representative of three independent experiments with cells. B, xCT relative mRNA levels of these cell lines were determined by real time PCR: delta-delta CT method. All mRNA expression levels were normalized to GAPDH. C, D, The THP-1 cells were pre-incubated for 2 hours in ACM, then resusupended with LPS (100 ng/mL) in 1 mL of ACM, L-Cys-free ACM and ACM plus L-Cys. The concentration of extracellular (C) and intracellular (D) amino acid was determined as described in material and methods. E, The CD14+ monocytes, cultured under ACM and ACM plus L-Cys for 24 hours, were harvested and labeled with antibodies (CD98, xCT or the relevant isotype controls). Using flow cytometry, surface marker expressions were analyzed. The figure expresses the mean fluorescence Intensity. Data shown are representative of three independent experiments with cells. F, Similarly as in Fig. 4C, the monocytes were cultured for 24 hours in ACM, L-Cys-free ACM and ACM plus L-Cys. The supernatants were measured by HPLC as extracellular amino acids quantification. G, Monocytes were pre incubated at a density of 2.0×10^5 cells/well in 96-well flat-bottom plates for 2 hours in HCM, and then cultured in HCM, ACM and ACM plus L-Cys (200 nmol/mL) for an additional 2 hours. These intracellular glutathione levels were measured by GSH-Glo™ at the time point indicated. C and D, Mean ± SD values from five independent experiments are shown. B *, $p<0.05$ vs Molt-4 (the Mann-Whitney U-test.). C,F **, $p<0.01$ *,$P<0.05$ (mean change vs ACM) D *, $p<0.05$ (paired Student's t test, two-tailed).
doi:10.1371/journal.pone.0023402.g003

differences between healthy controls and patients were analyzed by the Mann-Whitney U-test. All statistical analyses were performed with standard statistical software (SPSS 13.0 for Windows, Chicago, IL).

Results

The counts of peripheral monocytes were increased in association with the plasma L-Cystine in patients with advanced cirrhosis

Firstly, we confirmed that, in patients with advanced cirrhosis (Child-Pugh grade B or C), the plasma concentrations of L-Cys were significantly higher than in those with early cirrhosis (Figure 1A), and there was a wide range of variation. On the other hand, the plasma concentrations of L-Glu were significantly decreased along with the Child-Pugh grade (Figure 1B). In patients with advanced cirrhosis, the wide range of variation of L-Cys was attributed to the eGFR ($R^2 = 0.28/P = 0.0000008$) (Figure 1C). These data mean that plasma L-Cys increases in decompensated cirrhosis. Secondly, we investigate whether the concentration of plasma L-Cys influenced the peripheral monocyte counts. In patients with early cirrhosis, L-Cys was not correlated with the monocyte counts ($R^2 = 0.05/P = 0.119$) (Figure 1D), but in patients with advanced cirrhosis, it was significantly and positively correlated with the monocyte counts ($R^2 = 0.25/P = 0.0000017$) (Figure 1E). On the other hand, the lymphocyte counts were not correlated with the concentration of plasma L-Cys ($R^2 = 0.01/P = 0.523$) (Figure 1F). Interestingly, among all twenty kinds of free amino acids, only L-Cys was significantly correlated with the monocyte counts in patients with advanced cirrhosis (Figure S1). These data mean that, in patients with advanced cirrhosis, plasma L-Cys is increased according to renal dysfunction and influences the counts of monocytes.

Extracellular L-Cystine dose-dependently increased pro-inflammatory cytokines from CD14+ monocytes under the amino acid condition of advanced cirrhosis

Based on the result that the peripheral monocyte counts were positively correlated with the concentration of L-Cys, we hypothesized that the concentration of extracellular L-Cys could influence the proliferation of monocytes. To investigate this hypothesis, we cultured monocytes for 20 days with M-CSF under ACM or ACM plus L-Cys in vitro, and determined the proliferation of monocytes by CFSE assay. An elevated concentration of L-Cys did not influence the proliferation of monocytes (Figure 2A) on microscopic appearance, and also did not affect the morphological appearance and behavior of the cells in culture (Figure 2B). There was also no difference in the proliferation of the monocyte cell line, THP-1 between these media (data not shown). Next, to investigate whether the extracellular L-Cys level influenced the production of inflammatory cytokines from monocytes, we cultured monocytes under ACM that contained 50–300 nmol/mL L-Cys and measured the producton of TNF alpha from monocytes. The addition of L-Cys increased the production of TNF alpha from monocytes in a dose-dependent manner (Figure 2C), and the values were maximum under 150 nmol/mL L-Cys. Interestingly, this range was in remarkable agreement with the range in patients with advanced cirrhosis (Fig. 1A). The IL-10 level from monocytes was also significantly higher under ACM plus L-Cys than that under ACM (Figure 2D), and there was no difference the interferon gamma (IFN γ) level from monocytes between these media. The GM-CSF from PBMCs was also significantly higher under ACM plus L-Cys than that under ACM (Figure 2E). Regarding monocyte phenotypes, there was no difference between ACM and ACM plus L-Cys (Figure 2F). These data mean that high levels of extracellular L-Cys increased pro-inflammatory cytokines from CD14+ monocytes under the amino acid environment of patients with advanced cirrhosis.

High levels of extracellular L-Cystine promoted the L-Cystine-L-Glutamate antiport and decreased the intracellular GSH/GSSG ratio in monocyte under the amino acid environment of patients with advanced cirrhosis

We investigated whether high levels of extracellular L-Cys influence the L-Cys/L-Glu transport under the amino acid environment of patients with advanced cirrhosis.

Firstly, we determined the expression of 4F2hc (CD98) and xCT in THP-1, Jurkat and Molt-4. All cell lines expressed CD98, but only THP-1 expressed xCT at the protein level (Fig. 3A) and mRNA level (Fig. 3B). Secondly, we measured the intra-extracellular L-Cys and L-Glu concentration of THP-1 under ACM at various L-Cys levels. After 2 hours culture, ACM plus L-Cys significantly decreased the extracellular L-Cys (mean change, ACM+Cys, −96.8±15.8; ACM, −32.3±0.6 and ACM dep L-Cys, 4.8±6.6 nmol/mL) (Fig. 3C) and significantly increased intracellular L-Cys (Fig. 3D) and extracellular L-Glu (mean change, ACM+Cys, 157.5±19; ACM, 86.1±17.7 and ACM dep L-Cys, 40.4±24.9 nmol/mL) (Fig. 3C) more than that by ACM or ACM deprived of L-Cys. For intracellular L-Glu, there was no difference among these media. Such L-Cys/L-Glu changes were not seen for Jurkat and Molt-4 (data not shown). These data indicate that high levels of extracellular L-Cys enhances L-Cys/L-Glu antiport in the monocyte cell line THP-1. Similarly, CD14+ monocytes expressed CD98 and xCT after adding LPS (Fig. 3E) and extracellular L-Cys/L-Glu changes were seen (L-Cys mean change, ACM+Cys, −46.9±5.0; ACM, −22.4±6.0; ACM+Cys+Glu, −22.9±6.4 and

PBMC-CD14, −11.0±11.9 nmol/mL/L-Glu mean change; ACM+Cys, 70.4±24.8; ACM, 25.2±13.8 and PBMC-CD14, 10.7±7.0 nmol/mL) (Fig. 3F). Furthermore, we investigated whether high levels of extracellular L-Cys influence the intracellular glutathione level of monocytes. Interestingly, the intracellular GSH and GSH/GSSG ratio decreased more under ACM plus L-Cys than under ACM or HCM (Fig. 3G).

Plasma L-Cys/L-Glu ratio significantly correlated with plasma TNF-alpha level in patients with advanced cirrhosis

Finally, we actually measured the levels of TNF-alpha of patients with advanced cirrhosis in monocytes and plasma (Table S2). In patients with advanced cirrhosis (Table S2: patients 1–19), the TNF-alpha mRNA expression of monocytes was significantly

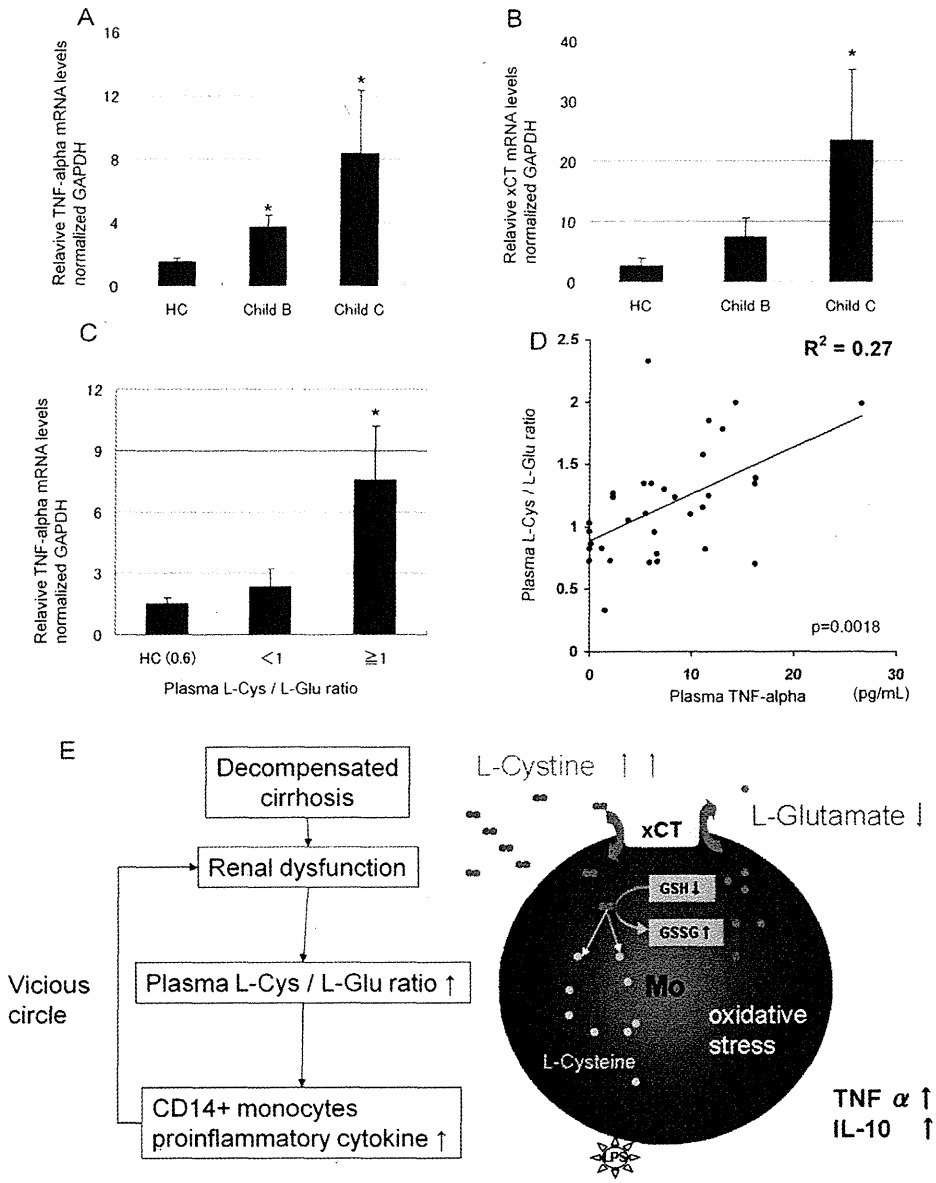

Figure 4. The plasma L-Cys/L-Glu ratio significantly correlated with the plasma TNF-alpha level in patients with advanced cirrhosis. A, CD14+monocytes were isolated from healthy volunteers (n = 5) and patients with adcanced cirrhosis (Table S2 : Patient 1–19). the TNF-alpha relative mRNA levels of CD14+monocytes were determined by real time PCR : delta-delta CT method. All mRNA expression levels were normalized to GAPDH. B, Similarly as in Fig. 4A, the xCT relative mRNA levels of monocytes were determined by real time PCR. C, These patients were separated into a high L-Cys/L-Glu ratio group (≧1) and low ratio group (<1). In healthy control (HC), the average plasma L-Cys/L-Glu ratio was 0.61±0.21. D, Linear regression model was used to model variation in plasma L-Cys/L-Glu ratio and plasma TNF-alpha. R^2 represents coefficient of determination. E, The schematic diagram of the present study concerning monocytes abnormality in patients with decompensated cirrhosis. A,B,C *, $p<0.05$ vs HC (the Mann-Whitney U-test.).

doi:10.1371/journal.pone.0023402.g004

higher than that of healthy controls (Fig. 4A), and xCT mRNA expressions also was increased according to the Child-pugh grade (Fig. 4B). Interestingly, the TNF-alpha mRNA of monocytes was significantly higher in the high plasma L-Cys/L-Glu ratio group (≥1) than in the low group (<1) (Fig. 4C). Consistent with these data, the plasma TNF-alpha in the patients was significantly correlated with the plasma L-Cys/L-Glu ratio ($p = 0.0018/r = 0.52247$) (Fig. 4D). We represented the schematic diagram of the present study concerning monocytes abnormality in patients with decompensated cirrhosis (Fig. 4E).

Discussion

Bacterial infections, such as spontaneous bacterial peritonitis (SBP) or pneumonia, are frequent clinical complications and causes of death in patients with advanced cirrhosis [20], because in such immune-compromised patients the innate immune cells can not normally respond to the pathogen [21]. Neutrophils, macrophages, and DCs are important cellular mediators of the innate immune defense. Circulating monocytes, however, are increasingly implicated as essential players in the defense against a range of microbial pathogens [22]. Previously, we made two serum-free media (HCM and ACM) to examine more closely the actual amino acid environment of the living body plasma [9]. First, we showed that plasma L-Cys was increased by renal dysfunction, which is an important factor of the MELD score [18], and showed a significantly positive correlation with the monocyte counts in patient with advanced cirrhosis. However, high levels of L-Cys did not directly influence the proliferation of monocytes in vitro. This paradox raises the possibility that the GM-CSF from PBMCs (Fig. 2E) may indirectly increase the peripheral monocyte counts, because the increase is almost entirely due to the release from bone marrow [23]. This issue should be evaluated in future studies. Second, we showed that extracellular L-Cys dose-dependently increases pro-inflammatory cytokines from monocytes with LPS under the amino acid environment of patients with advanced cirrhosis. Concerning the mechanism that underlies these phenomena, we confirmed that high extracellular levels of L-Cys enhanced the exchange L-Cys/L-Glu antiport of monocytes via xCT, and decreased the intracellular GSH/GSSG ratio under the amino acid condition of advanced cirrhosis. A previous study showed that oxidized Eh L-Cysteine/L-Cys induces the upregulation of nuclear factor-kappa B of monocytes in vitro [24]. These studies support our results. However, the same studies reported that the oxidized extracellular Cys/CySS redox state had no effect on cellular GSH/GSSG redox [24,25]. We think that such differences were probably caused by differences in the culture condition and stimulation period of the immune cells, and that our culture conditions more closely matched the actual amino acid environment of patients with advanced cirrhosis. However, we need to investigate in detail by separate quantification of the reduced form, L-Cysteine; the oxidized form, L-Cys; and the mixed protein L-Cysteine disulfide. Furthermore, we think that a low level of plasma L-Glu enhances the antiport in patients with advanced cirrhosis, because another study reported on a L-Cys transport system whose activity was inhibited by L-Glu in mammalian cultured cells [26].

Finally, we confirmed that the TNF-alpha mRNA of CD14 monocytes, isolated from patients with advanced cirrhosis, was at a higher level than in healthy controls. Furthermore, the value of plasma TNF-alpha showed a significantly positive correlating with the plasma L-Cys/L-Glu ratio.

This present results still cannot be construed as conclusive evidence of a change in the immune system in patients with advanced cirrhosis. We need to investigate whether L-Cys/L-Glu imbalance influences other immune cells such as macrophages, dendritic cells, T-cells and B-cells, and their interaction, and whether the level of L-Glu influences the immune system, because previous studies reported that glutamate is a immunomediator in the intercellular cross-talk between DC and T cells [12,14,27]. In conclusion, we demonstrated for the first time that an L-Cys/L-Glu imbalance, especially high levels of L-Cys, increases pro-inflammatory cytokines, especially TNF-alpha from peripheral CD14+ monocytes under the amino acid condition of advanced cirrhosis in vitro, and these results are consistent with the relationships among plasma L-Cys and TNF-alpha in patients with advanced cirrhosis. This study may provide a new approach for future studies to ameliorate the immune dysfunction in patients with advanced cirrhosis.

Supporting Information

Figure S1 Linear regression model was used to model variation in plasma L-Cys and monocyte count. Among all twenty kinds of free amino acids, only L-Cys was significantly correlated with the monocyte counts in patients with advanced cirrhosis.
(TIF)

Table S1 The serum free culture media used in this study. 'ACM (advanced cirrhotic medium) consistent with the average concentration of plasma amino acids from patients (Child-Pugh grade B or C, n = 90). ACM+Cys: Varying concentrations of L-Cys were added to L-Cys-free ACM, and the final concentration was adjusted to 100–300 nmol/mL. ACM dep Cys: L-Cys free ACM. Other components except amino acids, were identical among media. The amino acid concentrations are expressed in nmol/mL. Fischer's ratio = (Valine+Leucine+Isoleucine)/(Tyrosine+Phenylalanine). We verified that there was no difference between the theoretical value and actual value examined by high performance liquid chromatography.
(DOC)

Table S2 Characteristics of study participants. LC-C: liver cirrhosis due to HCV LC-B: liver cirrhosis due to HBV HCC: hepatocellular carcinoma PBC: Primary biliary cirrhosis Alcoholic: Alcoholic cirrhosis NASH: non alcoholic steatohepatitis HA: Hepatic Encephalopathy PLT: platelet counts ($\times 10^3/\mu L$) PT-INR: prothrombin time-international normalized ratio AST/ALT: aspartate amino transferase/alanine amino transferase (IU/L) Total Bilirubin (mg/dL) Albumin (g/dL) Fischer's ratio mean: L-Valine+L-Leucine+L-Isoleucine/L-Tyrosine+L-Phenylalanine.
(DOC)

Acknowledgments

We thank Dr. Hideyo Sato (University of Yamagata) for thoughtful discussions and Sonoko Ishizaki (Ajinomoto Pharmaceuticals Co) for helpful suggestions. We thank Takeshi Sato (Cell Science & Technology Institute, Inc, Sendai, Japan.) for providing the high quality serum free media. We thank Chikako Sato for excellent technical assistance.

Author Contributions

Conceived and designed the experiments: EK YU YK JI MN KF TS. Performed the experiments: EK YK JI MN OK YW. Analyzed the data: EK YU KF KT TS. Contributed reagents/materials/analysis tools: EK YU YK JI MN. Wrote the paper: EK YU YK TS.

References

1. Tilg H, Wilmer A, Vogel W, Herold M, Nolchen B, et al. (1992) Serum levels of cytokines in chronic liver diseases. Gastroenterology 103: 264–274.
2. Byl B, Roucloux I, Crusiaux A, Dupont E, Deviere J (1993) Tumor necrosis factor alpha and interleukin 6 plasma levels in infected cirrhotic patients. Gastroenterology 104: 1492–1497.
3. Riordan SM, Skinner N, Nagree A, McCallum H, McIver CJ, et al. (2003) Peripheral blood mononuclear cell expression of toll-like receptors and relation to cytokine levels in cirrhosis. Hepatology 37: 1154–1164.
4. Ubeda M, Munoz L, Borrero MJ, Diaz D, Frances R, et al. (2010) Critical role of the liver in the induction of systemic inflammation in rats with preascitic cirrhosis. Hepatology 52: 2086–2095.
5. Navasa M, Follo A, Filella X, Jimenez W, Francitorra A, et al. (1998) Tumor necrosis factor and interleukin-6 in spontaneous bacterial peritonitis in cirrhosis: relationship with the development of renal impairment and mortality. Hepatology 27: 1227–1232.
6. Gines P, Schrier RW (2009) Renal failure in cirrhosis. N Engl J Med 361: 1279–1290.
7. Morgan MY, Marshall AW, Milsom JP, Sherlock S (1982) Plasma amino-acid patterns in liver disease. Gut 23: 362–370.
8. Kakazu E, Kanno N, Ueno Y, Shimosegawa T (2007) Extracellular branched-chain amino acids, especially valine, regulate maturation and function of monocyte-derived dendritic cells. J Immunol 179: 7137–7146.
9. Kakazu E, Ueno Y, Kondo Y, Fukushima K, Shiina M, et al. (2009) Branched chain amino acids enhance the maturation and function of myeloid dendritic cells ex vivo in patients with advanced cirrhosis. Hepatology 50: 1936–1945.
10. Walshe JM, Senior B (1955) Disturbances of cystine metabolism in liver disease. J Clin Invest 34: 302–310.
11. Lemberg A, Fernandez MA (2009) Hepatic encephalopathy, ammonia, glutamate, glutamine and oxidative stress. Ann Hepatol 8: 95–102.
12. Pacheco R, Oliva H, Martinez-Navio JM, Climent N, Ciruela F, et al. (2006) Glutamate released by dendritic cells as a novel modulator of T cell activation. J Immunol 177: 6695–6704.
13. Eck HP, Droge W (1989) Influence of the extracellular glutamate concentration on the intracellular cyst(e)ine concentration in macrophages and on the capacity to release cysteine. Biol Chem Hoppe Seyler 370: 109–113.
14. D'Angelo JA, Dehlink E, Platzer B, Dwyer P, Circu ML, et al. (2010) The cystine/glutamate antiporter regulates dendritic cell differentiation and antigen presentation. J Immunol 185: 3217–3226.
15. Sato H, Shiiya A, Kimata M, Maebara K, Tamba M, et al. (2005) Redox imbalance in cystine/glutamate transporter-deficient mice. J Biol Chem 280: 37423–37429.
16. Sato H, Tamba M, Ishii T, Bannai S (1999) Cloning and expression of a plasma membrane cystine/glutamate exchange transporter composed of two distinct proteins. J Biol Chem 274: 11455–11458.
17. Matsuo S, Imai E, Horio M, Yasuda Y, Tomita K, et al. (2009) Revised equations for estimated GFR from serum creatinine in Japan. Am J Kidney Dis 53: 982–992.
18. Kamath PS, Wiesner RH, Malinchoc M, Kremers W, Therneau TM, et al. (2001) A model to predict survival in patients with end-stage liver disease. Hepatology 33: 464–470.
19. Dennis PB, Jaeschke A, Saitoh M, Fowler B, Kozma SC, et al. (2001) Mammalian TOR: a homeostatic ATP sensor. Science 294: 1102–1105.
20. Gustot T, Durand F, Lebrec D, Vincent JL, Moreau R (2009) Severe sepsis in cirrhosis. Hepatology 50: 2022–2033.
21. Galbois A, Thabut D, Tazi KA, Rudler M, Mohammadi MS, et al. (2009) Ex vivo effects of high-density lipoprotein exposure on the lipopolysaccharide-induced inflammatory response in patients with severe cirrhosis. Hepatology 49: 175–184.
22. Serbina NV, Jia T, Hohl TM, Pamer EG (2008) Monocyte-mediated defense against microbial pathogens. Annu Rev Immunol 26: 421–452.
23. Van Furth R, Diesselhoff-den Dulk MC, Mattie H (1973) Quantitative study on the production and kinetics of mononuclear phagocytes during an acute inflammatory reaction. J Exp Med 138: 1314–1330.
24. Go YM, Jones DP (2005) Intracellular proatherogenic events and cell adhesion modulated by extracellular thiol/disulfide redox state. Circulation 111: 2973–2980.
25. Iyer SS, Accardi CJ, Ziegler TR, Blanco RA, Ritzenthaler JD, et al. (2009) Cysteine redox potential determines pro-inflammatory IL-1beta levels. PLoS One 4: e5017.
26. Bannai S, Kitamura E (1980) Transport interaction of L-cystine and L-glutamate in human diploid fibroblasts in culture. J Biol Chem 255: 2372–2376.
27. Fallarino F, Volpi C, Fazio F, Notartomaso S, Vacca C, et al. (2010) Metabotropic glutamate receptor-4 modulates adaptive immunity and restrains neuroinflammation. Nat Med 16: 897–902.

JOURNAL OF VIRAL HEPATITIS
JVH

Journal of Viral Hepatitis, 2011, 18, 206–215 doi:10.1111/j.1365-2893.2010.01301.x

Four-year study of lamivudine and adefovir combination therapy in lamivudine-resistant hepatitis B patients: influence of hepatitis B virus genotype and resistance mutation pattern

J. Inoue, Y. Ueno, Y. Wakui, H. Niitsuma, K. Fukushima, Y. Yamagiwa, M. Shiina, Y. Kondo, E. Kakazu, K. Tamai, N. Obara, T. Iwasaki and T. Shimosegawa *Division of Gastroenterology, Tohoku University Graduate School of Medicine, Aoba-ku, Sendai, Japan*

Received September 2009; accepted for publication January 2010

SUMMARY. To investigate the efficacy of long-term lamivudine (3TC) and adefovir dipivoxil (ADV) combination therapy in 3TC-resistant chronic hepatitis B virus (HBV) infected patients, we analysed 28 3TC-resistant patients treated with the combination therapy during 47 months (range, 9–75). At 12, 24, 36, and 48 months, the rates of virological response with undetectable HBV DNA (≤2.6 log copies/mL) were 56, 80, 86, and 92%, respectively. Among 17 hepatitis B e antigen (HBeAg)-positive patients, HBeAg disappeared in 24% at 12 months, 25% at 24 months, 62% at 36 months, and 88% at 48 months. When HBV genotypes were compared, patients with genotype B achieved virological response significantly more rapidly than those with genotype C ($P = 0.0496$). One patient developed virological breakthrough after 54 months, and sequence analysis of HBV obtained from the patient was performed. An rtA200V mutation was present in the majority of HBV clones, in addition to the 3TC-resistant mutations of rtL180M+M204V. The rtN236T ADV-resistant mutation was observed in only 25% clones. *In vitro* analysis showed that the rtA200V mutation recovered the impaired replication capacity of the clone with the rtL180M+M204V mutations and induced resistance to ADV. Moreover, rtT184S and rtS202C, which are known entecavir-resistant mutations, emerged in some rtL180M+M204V clones without rtA200V or rtN236T. In conclusion, 3TC+ADV combination therapy was effective for most 3TC-resistant patients, especially with genotype B HBV, but the risk of emergence of multiple drug-resistant strains with long-term therapy should be considered. The mutation rtA200V with rtL180M+M204V may be sufficient for failure of 3TC+ADV therapy.

Keywords: chronic hepatitis B, drug resistance, HBV, rtA200V.

INTRODUCTION

Hepatitis B virus (HBV) causes acute and chronic infection, and chronic hepatitis often leads to liver cirrhosis and hepatocellular carcinoma (HCC) [1]. HBV contains a small (3.2 kb), circular, partially double-stranded DNA genome, and nucleoside or nucleotide analogues inhibit HBV replication by interfering with reverse transcriptase/DNA polymerase of the virus [2]. Although therapy with these drugs results in virological, biochemical, and histological improvement in most patients [3], the effect is often transient because of the emergence of drug-resistant HBV mutants [4].

Lamivudine (3TC), a nucleoside analogue of L-deoxycitydine, is associated with highly frequent emergence of drug-resistant mutants: the cumulative rate is about 20% per year [5,6]. Mutations that result in the replacement of methionine at amino acid 204 to valine or isoleucine (rtM204V/I) within the tyrosine-methionine-aspartate-aspartate (YMDD) motif in the reverse transcriptase (RT) region of HBV polymerase are found in most of the 3TC-resistant isolates [7]. Compensatory mutations rtV173L and rtL180M, which restore the replication capacity of the YMDD mutant *in vitro*, are observed frequently together with the YMDD mutation [8,9]. Adefovir dipivoxil (ADV) is a phosphonate nucleotide analogue of adenosine monophosphate, and ADV-resistance rates are lower than those of 3TC [10]. Two mutations, rtA181V/T and rtN236T, are associated with resistance to ADV [11–14], and the cumulative 5-year occurrence of genotypic resistance is reported to be 29% [15]. *In vitro* studies showed that these mutations confer a weaker

Abbreviations: ADV, adefovir dipivoxil; ALT, alanine aminotransferase; eGFR, estimated glomerular filtration rate; ETV, entecavir; HBeAg, hepatitis B e antigen; HBsAg, hepatitis B surface antigen; HBV, hepatitis B virus; HCC, hepatocellular carcinoma; PCR, polymerase chain reaction; RT, reverse transcriptase; TDF, tenofovir disoproxil fumarate.

Correspondence: Yoshiyuki Ueno, Division of Gastroenterology, Tohoku University Graduate School of Medicine, 1-1 Seiryo, Aoba-ku, Sendai 980-8574, Japan. E-mail: yueno@mail.tains.tohoku.ac.jp

decrease in the susceptibility to ADV, in comparison with the greater decrease in 3TC susceptibility because of the YMDD mutant [11,16]. This finding may explain the lower rate of the emergence of ADV resistance.

Although the number of approved drugs has increased in recent years, the treatment of chronic HBV infection remains a clinical challenge. Especially, how to manage drug-resistant patients including 3TC-resistant patients is a major problem. Continuation of 3TC monotherapy or retreatment with 3TC after its temporary discontinuation is ineffective options for 3TC-resistant patients [17]: the lack of any further benefit and the possibility of rapid re-emergence of resistant HBV have been reported [18]. Against 3TC-resistant HBV, ADV and entecavir (ETV) have a suppressive effect *in vivo* and *in vitro* [19–21]. Combination therapy of ADV and 3TC is effective for 3TC-refractory patients and has a low frequency of viral breakthrough [22]: the 3-year cumulative rate of *de novo* resistant mutants was 4% with no development of viral breakthrough in 3TC-resistant patients. However, further longer-term efficacy of the combination therapy remains unknown. ETV is a potent drug with infrequent development of resistance for treatment-naïve patients [23]. ETV monotherapy was shown to be effective during the first year of therapy in 3TC-resistant patients [20], but pre-existing 3TC-resistant mutants are favourable for the emergence of ETV resistance [21], and a comparatively high rate of the emergence of ETV-resistant strains has been reported in long-term studies [23]. Therefore, ETV monotherapy seems to be a less attractive option for the long-term treatment of 3TC-resistant patients.

Several previous reports have described the differences in the responses to antiviral therapy between HBV genotypes. A case–control study of 3TC treatment for genotypes B and C showed that the responses were not different, but the emergence of the YMDD mutation was more frequent in genotype C [24]. It was also reported that the YMDD mutation and breakthrough hepatitis developed more often in patients with genotype A than in patients with genotype B or C [25]. However, the impact of the genotype on the efficacy to ADV is uncertain.

Here, we studied the long-term efficacy of 28 3TC-resistant patients treated with the combination of 3TC and ADV and compared the response between HBV genotypes. Sequence analysis of HBV from a patient with resistance to the combination therapy was performed, and *in vitro* drug susceptibility of the mutant HBV clones was assessed to clarify the mechanism of the emergence of resistance.

MATERIALS AND METHODS

Patients

A total of 28 consecutive Japanese patients with chronic HBV infection who were treated with 3TC+ADV at Tohoku University Hospital from June 2003 to August 2009 for more than 6 months were enrolled in this study. All patients developed virological breakthrough during 3TC monotherapy, and ADV was added in. Virological breakthrough was defined as an increase in the serum HBV DNA level of ≥1 log copies/mL, which was determined using the Amplicor HBV monitor test (Roche Diagnostics, Tokyo, Japan), at two or more consecutive examinations in comparison with the lowest level after treatment. To evaluate renal function, the estimated glomerular filtration rate (eGFR) level using the Cockcroft-Gault formula [(140 - age) × (weight in kilograms) × (0.85 if female)/(72 × serum creatinine)] [26] was calculated. No patients were infected with HCV, nor had a history of other liver diseases. The patients were evaluated for the rate of virological response (undetectable HBV DNA: <2.6 log copies/mL), biochemical response [alanine aminotransferase (ALT) normalization: ≤35 IU/L], hepatitis B e antigen (HBeAg) loss, and virological breakthrough.

Antiviral treatment

Adefovir dipivoxil was administered at a dosage of 10 mg/day in all but one patient in addition to 3TC at a dosage of 100 mg/day. One patient received 10 mg of ADV on alternate days and 50 mg/day of 3TC daily because of reduced eGFR at the start of treatment. This occurred when the eGFR level dropped to <50 mL/min.

Determination of HBV genotype

The HBV genotype was determined as described previously [27] with minor modifications. Briefly, total DNA was extracted from 50 μL of serum sample by QIAamp Blood Mini kit (QIAGEN GmbH, Hilden, Germany) and subjected to nested polymerase chain reaction (PCR) with high fidelity polymerase (PrimeSTAR HS DNA polymerase; TaKaRa Bio Inc., Shiga, Japan), to amplify a 396-nt sequence in the S gene. The amplification products were sequenced on both strands directly using the BigDye Terminator v3.1 Cycle Sequencing kit on an ABI PRISM 3100 Genetic Analyzer (Applied Biosystems, Foster City, CA, USA). Sequence analysis was performed using Genetyx-Mac (Version 12.2.7; Genetyx Corp., Tokyo, Japan). The genotype of HBV was determined by phylogenetic analysis with HBV isolates whose genotype was known.

Sequencing analysis of HBV reverse transcriptase region

Total DNA extracted from 50 μL of serum sample was subjected to nested PCR to amplify the 1148-nt sequence [nt 52 to 1199, the nucleotide numbers are in accordance with a genotype C HBV isolate of 3,215 nt (AB033550)] including the RT region of HBV polymerase. The first-round PCR was carried out with primers B026 [5′-TCA TCC WCA GGC CAT GCA GTG GA-3′ (W = A or T)] and B025 (5′-CTA GGA GTT CCG CAG TAT GGA TCG-3′), and the second round with

primers B011 [5′-YTT YCC TGC TGG TGG CTC CAG TTC-3′ (Y = C or T)] and B024 (5′-GGG GTT GCG TCA GCA AAC ACT TG-3′). The amplification products were sequenced on both strands directly or after cloning into pUC118. Sequencing analysis after cloning was performed at nt 497-1161.

Construction of plasmid

A cloned mutant sequence including the RT region from a sample obtained after the development of 3TC and ADV resistance was digested with BlnI (TaKaRa Bio Inc.) and EcoT22I (TaKaRa Bio Inc.). The digested fragment (nt 179-1068) was ligated into the BlnI-EcoT22I site of pBFH2R, which contained a 1.3-fold HBV genome [28]. Quick Change II-E Site-Directed Mutagenesis kit (Stratagene, La Jolla, CA, USA) was used to introduce nucleotide substitutions into the plasmid. Each mutation found in the RT region, rtL180M [C to A at nt 667 (C667A)], rtT184S (A679T), rtA200V (C728T), rtS202C (A733T), rtM204V (A739G), and rtN236T (A836C), was converted into the wild type or another mutant nucleotide. To construct plasmids with combined nucleotide substitutions, these converted plasmids were used next as templates. As a result, variant constructs harbouring rtM204I, rtL180M+M204V, rtL180M+T184S+M204V, rtL180M+A200V+M204V, rtL180M+S202C+M204V, rtL180M+M204V+N236T, and rtL180M+A200V+M204V+N236T were composed, and all constructs were sequenced to confirm the nucleotide substitutions.

Cell culture and transfection

Human hepatoma HepG2 cells were cultured in Dulbecco's modified Eagle medium supplemented with 10% bovine serum at 37 °C and 5% CO_2. Cells were seeded in 24-well plates at 1.25×10^5 cells/well. On the next day, 375 ng of plasmid DNA were transfected into these cells using TransIT LT-1 Transfection Reagent (Mirus, Madison, WI, USA), and cells were washed twice with phosphate-buffered saline after 4 h. Five hundred microliter of the medium and various amounts of adefovir (Toronto Research Chemicals Inc., Ontario, Canada) were added, and the culture supernatant was collected 4 days later. Experiments were performed at least in triplicate.

Real-time PCR and determination of IC_{50}

HBV DNA in the culture supernatant was quantified by real-time PCR as described previously [28] to determine the 50% inhibitory concentration (IC50) for ADV of each mutant HBV clone. Briefly, to digest the input plasmid DNA in the culture supernatant, 5 μL of the supernatant were treated with 5 units of DNase I (TaKaRa Bio Inc.) at 37 °C for 2 h, and the reaction was stopped with EDTA. Then, total DNA was extracted with a QIAamp DNA Blood Mini kit, and 10 μL of 200 μL DNA solution were subjected to real-time PCR using a LightCycler (Roche Diagnostics). Dose–response curves were plotted to determine the ADV IC50.

Statistical analysis

Statistical analyses were performed using Fisher's exact probability test for comparison of proportions between two groups and Mann–Whitney *U* test for comparison of continuous variables between two groups. The cumulative rate of undetectable HBV DNA or ALT normalization was calculated using the Kaplan–Meier method, and differences between the curves were tested using Log-rank test. Differences were considered to be statistically significant when $P < 0.05$.

RESULTS

Study profile

The demographic and clinical profiles of the 28 patients [20 men and 8 women, median age 53.5 years (range 18–72)] at commencement of 3TC+ADV therapy are shown in Table 1. One (3.6%), 7 (25.0%), and 19 (67.9%) patients had HBV of genotypes A, B, and C, respectively. Eight (28.6%) patients had cirrhosis, 7 (25.0%) had HCC, and 17 (60.7%) patients were HBeAg positive. The mutations of the YMDD motif were determined by direct sequencing, and the YIDD, YVDD, and YIDD+YVDD mixed pattern were found in 14 (50%), 11 (39%), and 2 (7%)of the patients, respectively. Only one (4%) patient had no mutation in the YMDD motif. There were no significant differences in the profiles between patients with genotype B and those with genotype C.

Response to lamivudine and adefovir dipivoxil combination therapy

The 3TC-resistant patients treated with the combination therapy were followed up for a median of 47 months (range, 9–75). All patients continued to be treated with 3TC and ADV until virological breakthrough. The 6-, 12-, 24-, 36-, and 48-month rates of virological response with HBV DNA ≤ 2.6 log copies/mL were 39, 56, 80, 86, and 92%, respectively (Table 2). The ALT normalization rates were 57% at 6 months, 70% at 12 months, 84% at 24 months, 82% at 36 months, and 77% at 48 months. When compared between genotype B and C, the results of patients with genotype B tended to be favourable for both virological and biochemical response (Figs 1a,b). The cumulative probability of undetectable HBV DNA was significantly higher in genotype B than in genotype C ($P = 0.0496$), whereas there was no significant difference in that of ALT normalization. Notably, patients with genotype B achieved early virological response (HBV DNA < 2.6 log copies/mL at 6 months) significantly more frequently than those with genotype C

Table 1 Demographic and clinical characteristics of the 28 lamivudine-resistant patients at the start of adefovir addition to the treatment

	Overall (n = 28)*	Genotype B (n = 7)	Genotype C (n = 20)
Age (years), median (range)	53.5 (18–72)	51.0 (18–72)	53.5 (35–68)
Male patients, no. (%)	20 (71.4)	5 (71.4)	14 (70.0)
Patients with cirrhosis, no. (%)	8 (28.6)	1 (14.3)	7 (35.0)
Patients with HCC, no. (%)	7 (25.0)	0 (0)	7 (35.0)
HBeAg positive, no. (%)	17 (60.7)	3 (42.9)	13 (65.0)
HBV DNA (log copies/mL), median (range)	7.6 (4.3 to >7.6)	7.2 (5.3 to >7.6)	7.6 (4.3 to >7.6)
Patients with rtM204 mutation (M:I:V:I/V, no.)	1:14:11:2	1:3:2:1	0:11:8:1
ALT (IU/L), median (range)	86.5 (29–1027)	314.0 (47–760)	78.5 (29–1027)
T. Bil (mg/dL), median (range)	1.1 (0.5–4.5)	1.1 (0.5–1.5)	1.1 (0.5–4.5)
Albumin (g/dL), median (range)	4.1 (2.7–4.8)	4.2 (3.8–4.8)	4.0 (2.7–4.6)
Serum creatinine (mg/dL), median (range)	0.7 (0.4–1.2)	0.7 (0.6–1.2)	0.7 (0.4–1.2)
Prior lamivudine therapy (month), median (range)	28.6 (2–76)	36.5 (2–76)	28.6 (5–65)

HCC, hepatocellular carcinoma; ALT, alanine aminotransferase; T. Bil, total bilirubin. *One patient had genotype A HBV.

Table 2 Virological and biochemical response to lamivudine and adefovir combination therapy during a median of 47 months

	Months of treatment						
Response	0 (n = 28)	6 (n = 28)	12 (n = 27)	24 (n = 25)	36 (n = 22)	48 (n = 13)	60 (n = 7)
HBV DNA < 2.6	0 (0)	11 (39.3)	15 (55.6)	20 (80.0)	19 (86.4)	12 (92.3)	6 (85.7)
HBV DNA 2.6 to <5.0	1 (3.6)	15 (53.6)	11 (40.7)	5 (20.0)	3 (13.6)	1 (7.7)	1 (14.3)
HBV DNA ≥ 5.0	27 (96.4)	2 (7.1)	1 (3.7)	0 (0)	0 (0)	0 (0)	0 (0)
ALT normalization*	NA	16 (57.1)	19 (70.4)	21 (84.0)	18 (81.8)	10 (76.9)	6 (85.7)
HBeAg disappearance†	NA	1/17 (5.9)	4/17 (23.5)	4/16 (25.0)	8/13 (61.5)	7/8 (87.5)	4/5 (80.0)
Virological breakthrough	NA	0 (0)	0 (0)	0 (0)	0 (0)	0 (0)	1 (14.3)

Values are shown as numbers of patients followed by percentages in parentheses. NA, not applicable. *ALT ≤ 35 IU/L. †Values are shown as numbers of patients/total followed by percentages in parentheses.

[5/7 (71%) vs. 5/20 (25%), P = 0.0427]. Although the status of HBeAg at the start of ADV seemed to influence the response, the difference was not significant (Figs 1c,d). Among 17 HBeAg-positive patients, HBeAg disappeared in 6% at 6 months, 24% at 12 months, 25% at 24 months, 62% at 36 months, and 88% at 48 months. There was no patient with hepatitis B surface antigen (HBsAg) loss during follow-up in this study.

Three of 22 patients who were treated for more than 36 months did not achieve virological response. One of them developed virological breakthrough after 54 months of combination therapy. The other patients had 2.8 and 3.5 log copies/mL of serum HBV DNA at 36 months of therapy but did not develop breakthrough. None of the patients experienced biochemical breakthrough. One patient with HCC died of HCC progression at 9 months after ADV. None of the 21 patients without HCC at the start of ADV developed HCC during follow-up.

The renal toxicity with a ≥0.3 mg/dL increase in serum creatinine level was observed in five of the 28 patients. Two of them had a ≥0.5 mg/dL increase: the serum creatinine levels were increased from 0.8 to 1.4 mg/dL after 31 months in a patient, and from 0.9 to 1.7 mg/dL after 34 months in another patient. As their eGFR levels were lowered to 39 and 29 mL/min, the dosage of ADV was reduced to alternate-day administration. After the reduction of ADV, their serum creatinine and eGFR recovered.

Profile of a patient with lamivudine and adefovir dipivoxil resistance

He was a 53-year-old Japanese man with HBeAg-positive liver cirrhosis at the start of 3TC monotherapy in April 2002. The genotype of HBV was found to be genotype C. His clinical course is shown in Fig. 2. He developed breakthrough hepatitis with serum HBV DNA of >7.6 log copies/mL and alanine aminotransferase (ALT) of 236 IU/L in March 2003. ADV was added to the ongoing 3TC therapy in June 2003, and HBV DNA was gradually reduced reaching <2.6 log copies/mL 3 years later. However, virological

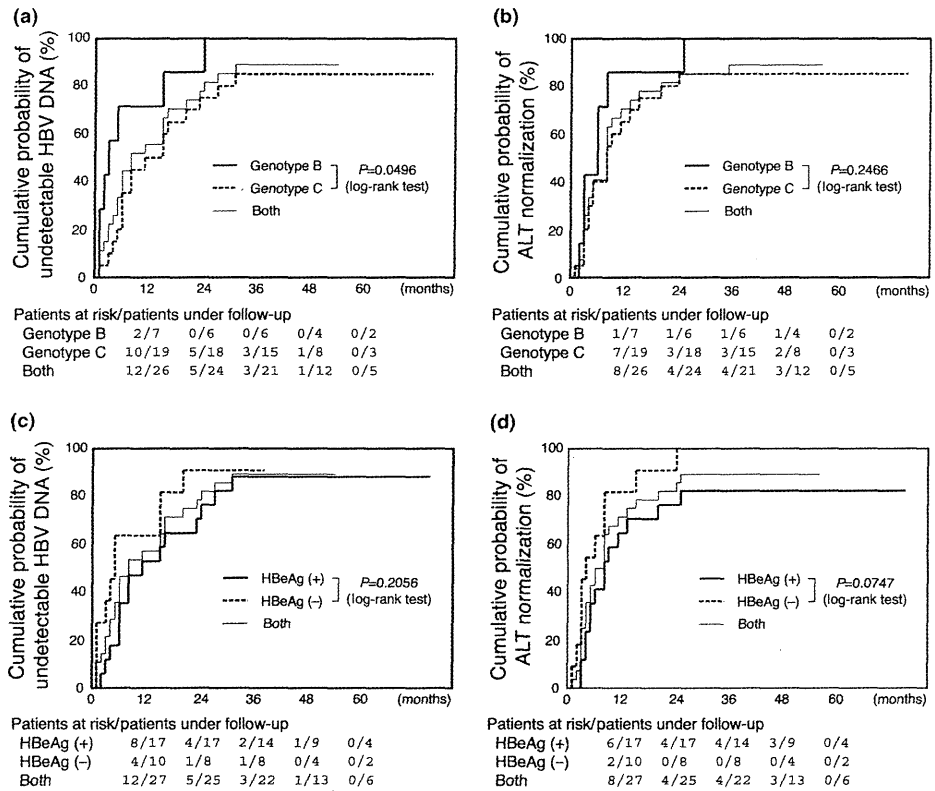

Fig. 1 Cumulative probability of virological or biochemical response during lamivudine (3TC) and adefovir dipivoxil (ADV) combination therapy. (a) Cumulative probability of undetectable HBV DNA (<2.6 log copies/mL) in patients with genotype B and those with genotype C. (b) Cumulative probability of ALT normalization (≤35 IU/L) in patients with genotype B and those with genotype C. (c) Cumulative probability of undetectable HBV DNA in HBeAg-positive patients and HBeAg-negative patients. (d) Cumulative probability of ALT normalization in HBeAg-positive patients and HBeAg-negative patients.

breakthrough was observed at 4 years after starting ADV, and his HBV DNA reached 4.3 log copies/mL in December 2007. Because his liver was cirrhotic and the hepatic functional reserve was impaired, combination therapy of tenofovir disoproxil fumarate (TDF) and 3TC was started before ALT flair. Two months later, his HBV DNA was suppressed to <2.6 log copies/mL, and viral breakthrough has not been observed to date (20 months later).

Mutations found in the HBV reverse transcriptase region of the lamivudine and adefovir dipivoxil-resistant patient

To investigate the mutations responsible for the viral breakthrough during the 3TC and ADV combination therapy, nucleotide sequences of the HBV RT region of the patient were compared between 3 time points: at the beginning of ADV treatment, at 30 months after ADV therapy, and at the time of viral breakthrough (54 months after ADV therapy). Direct sequencing analysis showed 10 amino acid changes during the clinical course (Fig. 2). The 3TC-resistant mutation of rtM204I changed to rtM204V after ADV treatment. Along with the change, the mixed mutation of rtL180L/M changed to rtL180M, which was reported to emerge with rtM204V during 3TC therapy [9]. The rtN236T mutation, which is a known ADV-resistance mutation [11], emerged as a mixed mutation with wild type (rtN236N/T) after viral breakthrough. Notably, rtA200V, which has never been reported as an ADV-resistant mutation, emerged also after viral breakthrough as a mixed mutation (rtA200V/A). Meanwhile, no specific mutation was found in the 2 patients without virological breakthrough who did not achieve virological response after 3 years of the combination therapy.

Clonal analysis was performed to examine the significance of these mutations of the RT region (Table S1). Several minor mutations were found during the 3TC and ADV therapy. After viral breakthrough, rtA200V was found in 63% of the clones, while rtN236T was found in only 25% of the clones. Therefore, rtA200V seemed to be responsible for the treatment failure of ADV. Moreover, rtT184S and S202C, which were reported as ETV resistance–associated mutations [29], were found as a minor population.

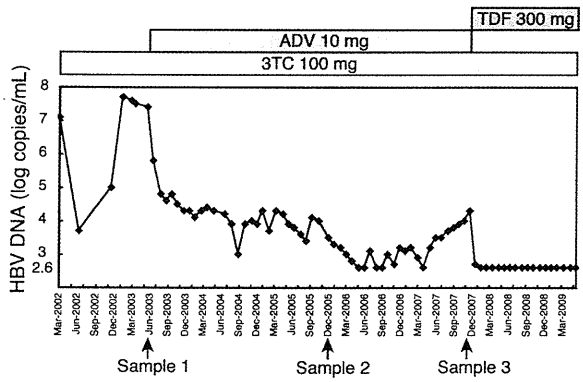

RT mutation	L80	P109	D134	R153	L180	A200	M204	V214	L229	N236
Sample 1	I/L	P/Q	G/D	R/Q	L/M	–	I	–	L/W	–
Sample 2	–	–	–	–	M	–	V	A	–	–
Sample 3	–	–	G/D	–	M	V/A	V	–	–	N/T

Fig. 2 Clinical course of a lamivudine (3TC)-resistant patient who developed virological breakthrough during 3TC and adefovir dipivoxil (ADV) combination therapy, and changes of amino acids in the reverse transcriptase (RT) region detected by direct sequencing analysis. After breakthrough, therapy was switched to 3TC plus tenofovir disoproxil fumarate (TDF) combination. The arrows indicate the time point when serum samples were obtained for sequencing analysis. Sample 1, 2, and 3 were obtained at the start of ADV, 30 months after ADV, and 54 months after ADV, respectively.

To investigate further the mutant populations, the combinations of these mutations and 3TC-resistant mutations were analysed (Fig. 3). At 30 months after ADV therapy, 100% of clones had mutations rtL180M+M204V. Subsequently, the mutations of rtT184S, A200V, S202C, and N236T emerged in the rtL180M+M204V clones after viral breakthrough. Of note, rtN236T was not found in clones without rtA200V.

Replication capacity and drug susceptibility of HBV mutants

We analysed the replication capacity of HBV clones with combined mutations as shown in Fig. 3. A clone with rtL180M+M204V+N236T mutations, which was not found in the patient, was also included for comparison. Consistent with a previous report [30], 3TC-resistant mutations of rtM204I or rtL180M+M204V lowered the replication capacity significantly in comparison with the wild-type clone (Table 3). From additional mutations to rtL180M+M204V found in the patient, only rtA200V restored the impaired replication capacity significantly. The ETV-resistant mutation of rtT184S and rtS202C did not seem to have such an effect. The ADV-resistant mutation, rtN236T, lowered the replication capacity further, and rtA200V did not restore the lowered capacity caused by rtN236T.

The 7 HBV clones with mutations in the RT region were analysed for their susceptibility to ADV. The IC_{50} of each clone is shown in Table 3. The clones with the 3TC-resistant mutations of rtM204I or rtL180M+M204V showed moderate resistance to ADV. In comparison with the clone with rtL180M+M204V, clones with additional mutations of rtT184S, A200V, or S202C showed significantly higher resistance to ADV. An additional mutation of rtN236T led to much greater resistance to ADV. Taking into account the results from the clonal analysis of serum samples and the replication capacity of each clone, rtA200V may be responsible for the treatment failure of 3TC+ADV therapy when it presents with 3TC-resistant mutations such as rtL180M+M204V. The mutations of rtT184S or S202C with rtL180M+M204V also confer ADV resistance, but the clones

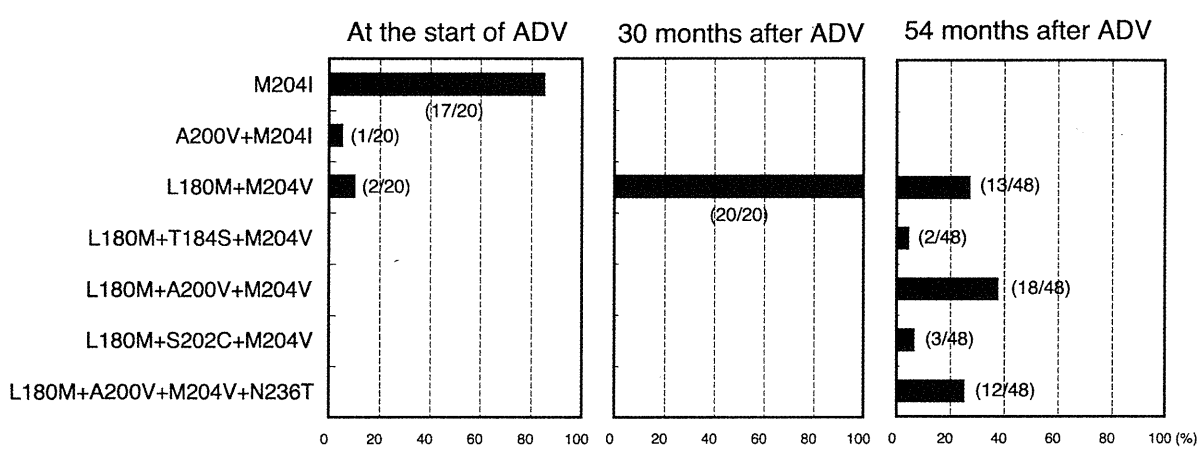

Fig. 3 Clonal analysis of HBV obtained from the patient with 3TC and ADV resistance. The serum samples were collected at the time points indicated in Fig. 2. The percentages (no. of clones/total in parentheses) of the clones with the combined mutations in the RT region are shown.

Table 3 Replication capacity and susceptibility to adefovir of the HBV mutants

HBV mutants	HBV DNA ($\times 10^7$ log copies/mL)*	Fold replication†	IC_{50} (μM)*	Fold resistance†
Wild type	13.60 ± 3.50	1	0.42 ± 0.06	1
M204I	2.17 ± 0.38	0.16	0.87 ± 0.2	2.07
L180M+M204V	4.38 ± 0.77	0.32	0.73 ± 0.06	1.74
L180M+T184S+M204V	5.98 ± 0.80	0.44	0.91 ± 0.04	2.17‡
L180M+A200V+M204V	8.90 ± 0.56	0.65‡	1.09 ± 0.12	2.60‡
L180M+S202C+M204V	4.86 ± 0.19	0.36	2.19 ± 0.63	5.21‡
L180M+M204V+N236T	0.88 ± 0.68	0.07‡	>10	>25
L180M+A200V+M204V+N236T	0.54 ± 0.38	0.04‡	>10	>25

*Values are expressed as means ± SD of experiments performed in triplicate. †(Mean value of the mutant)/(mean value of the wild type). ‡$P < 0.05$ in comparison with the clone with rtL180M+M204V.

with these mutations were not major, because they had no effect in enhancing the replication capacity of HBV.

DISCUSSION

As clinical and histological improvement accompanies reductions in HBV replication, therapies that reduce HBV replication are expected to limit the progression of liver disease and improve the natural history of chronic HBV infection [10]. Currently, the management of hepatitis B patients with drug resistance is one of the major problems in clinical practice for hepatitis B. A substantial part of 3TC-treated patients has mutant HBV with the YMDD mutation, and several clinical trials to treat 3TC-resistant hepatitis B have been performed. It has been reported first that with ADV alone and in combination with 3TC, the viral and biochemical responses were the same for 3TC-resistant patients in a 1 year study [31]. However, several studies of longer term treatment have shown that adding ADV was superior to switching to ADV monotherapy for patients with 3TC resistance [32–34]. In this study, we demonstrated that the add-on ADV therapy for 3TC-resistant hepatitis B patients effectively suppressed serum HBV DNA for a median of 47 months. Moreover, the biochemical response of ALT normalization was achieved in 77% patients and HBeAg loss in 88% of the HBeAg-positive patients at 48 months. The undetectability of HBV DNA was assessed by the Amplicor HBV monitor test, but recently, this can be assessed by a more sensitive real-time assay such as the Cobas TaqMan HBV test (Roche Diagnostics). The treatment duration to achieve HBV DNA undetectability might be longer if a more sensitive assay was used.

The influence of HBV genotype on the response or resistance to ADV has not been clarified, whereas the efficacy to 3TC was reported to be different between HBV genotypes [24,25]. This study showed that the virological response to 3TC+ADV was significantly earlier in genotype B than in C. However, there were several limitations of the results: the patients with genotype B were fewer, and no multivariate analysis was performed. In addition, all patients with HCC were genotype C, and ALT levels of genotype B tended to be higher, although there were no significant differences. The effect of genotype on the response to 3TC±ADV should be confirmed in larger studies. The baseline HBeAg status in 3TC+ADV combination therapy in 3TC-resistant patients was reported to influence the viral response: HBeAg-negative patients showed better virological and biological response [35]. In this study, the same tendency was observed, but the difference was not significant.

Initial virological suppression by ADV monotherapy was reported to be a good prognostic factor for the treatment of both naïve patients [36] and 3TC-resistant patients [37]. Taking into account the results of this study and previous reports, it is suggested that patients with genotype B HBV might develop resistance to 3TC+ADV less frequently than those with genotype C. In fact, the 3TC+ADV-resistant patient in this study was infected with genotype C HBV. Because the development of resistance to 3TC+ADV combination therapy is rare [22,35], it is difficult to evaluate whether the early virological response or genotype B is associated with the lower frequency of resistance to 3TC+ADV combination therapy. Further long-term study is needed to clarify this issue.

Although the emergence of resistance in this study was rare during the combination therapy as previously reported [22,35], one patient developed virological breakthrough after 4.5 years. We identified a characteristic mutation pattern of HBV in this patient. The mutation of rtA200V rescued the *in vitro* replication capacity that was impaired by rtL180M+M204V and reduced the susceptibility to ADV. In previous reports, rtA200V emerged as an additional mutation with the 3TC-resistant mutation in patients under 3TC monotherapy [38,39]. The effect of this mutation is not as strong as the effect of rtM204I/V±L180M on 3TC susceptibility *in vitro*, which showed >1000-fold resistance [40]. However, the clinical dose of ADV is comparatively low

because of renal toxicity [41], and the weakly resistant profile *in vitro* can explain the great clinical impact. Villet *et al.* reported that rtA200V was observed in a patient with 3TC monotherapy, and it was no longer detected after the combination therapy with ADV and 3TC [39]. The difference of results between the previous study and our study may be because of the emergence of mutations with a potent effect on ADV resistance, such as rtV173L and rtA181V, in the previous study. Because these mutations may have a greater effect on ADV resistance than rtA200V, the HBV clones with rtA200V seemed to disappear in the previous study case.

The known ADV-resistant mutation of rtN236T was found in only 25% clones, exclusively with rtA200V. This may indicate that rtN236T appeared after the emergence of rtA200V. In the active replication of the clones with rtA200V, which restored the replication capacity and enhanced ADV resistance, other mutations including rtN236T might occur more readily.

The rtA200V mutation is the result of nucleotide substitution C728T. This change in the overlapping S region results in an amino acid substitution affecting HBsAg: Leu to Phe at aa192 (sL192F). There is a possibility that sL192F may affect the replication capacity of HBV, but the actual mechanism is unknown.

Interestingly, the ETV-resistant mutations of rtT184S and rtS202C were also detected during 3TC+ADV combination therapy by clonal analysis. These mutations confer ETV resistance in the presence of the 3TC-resistant mutations of rtM204I/V±L180M [21]. This study showed that these mutations also have an ADV-resistance profile. These mutations may not cause viral breakthrough, because the population of these mutants in the patient was minor (4% and 6%, respectively), and their replication capacity was lower than that with rtA200V *in vitro*. The emergence of these mutations suggested that long-term 3TC+ADV therapy has the possibility of leading to multiple drug resistance including ETV resistance.

The combination therapy of 3TC and ADV is very effective with little frequency of viral breakthrough for 3TC-refractory patients. However, some patients do not achieve complete viral suppression of serum HBV DNA to under 2.6 log copies/mL. It was considered that the incomplete suppression of viral replication might favour further selection of drug-resistant mutants [42]. Although there have been a few reports of cases that showed resistance to 3TC+ADV therapy to date, the number of resistant cases will increase along with the increase in cases with long-term therapy. The 3TC- and ADV-resistant patient in this study was treated with 3TC and TDF after the virological breakthrough, and HBV DNA was promptly suppressed. Although TDF was reported to show cross-resistance with ADV *in vitro* [16,40,43], there are several reports that showed the effectiveness of TDF for ADV-refractory patients [44–46]. It is thought that the potency of TDF might result from its higher clinical dose compared to that of ADV [47].

In conclusion, this study showed that the combination therapy of 3TC and ADV effectively suppressed HBV replication in 3TC-resistant patients with chronic HBV infection for 4 years. Especially, patients with genotype B achieved earlier virological response than those with genotype C. However, one of the 28 patients developed virological breakthrough during the combination therapy over 4 years, and the HBV mutation of rtA200V, in addition to 3TC-resistant mutations, was demonstrated to contribute to the ADV resistance. Moreover, ETV-resistant mutations emerged coincidentally in minor HBV clones. The risk of emergence of multiple drug-resistant mutant should be considered in cases with long-term therapy with nucleos(t)ide analogues, especially when serum HBV DNA cannot be suppressed completely. Potent antiviral agents should be administered in such cases to prevent the emergence of multiple drug-resistant HBV mutants that are difficult to treat.

ACKNOWLEDGEMENTS

This study was supported in part by Grant-in-Aid for Young Scientists (B) (assignment no. 20790483) from Ministry of Education, Culture, Sports, Science, and Technology of Japan, and by grants from Ministry of Health, Labor, and Welfare of Japan.

REFERENCES

1 Ganem D, Prince AM. Hepatitis B virus infection – natural history and clinical consequences. *N Engl J Med* 2004; 350: 1118–1129.
2 Doong SL, Tsai CH, Schinazi RF, Liotta DC, Cheng YC. Inhibition of the replication of hepatitis B virus in vitro by 2′,3′-dideoxy-3′-thiacytidine and related analogues. *Proc Natl Acad Sci U S A* 1991; 88: 8495–8499.
3 Lai CL, Chien RN, Leung NW *et al.* A one-year trial of lamivudine for chronic hepatitis B. Asia Hepatitis Lamivudine Study Group. *N Engl J Med* 1998; 339: 61–68.
4 Ling R, Mutimer D, Ahmed M *et al.* Selection of mutations in the hepatitis B virus polymerase during therapy of transplant recipients with lamivudine. *Hepatology* 1996; 24: 711–713.
5 Lai CL, Dienstag J, Schiff E *et al.* Prevalence and clinical correlates of YMDD variants during lamivudine therapy for patients with chronic hepatitis B. *Clin Infect Dis* 2003; 36: 687–696.
6 Zoulim F. Hepatitis B virus resistance to antivirals: clinical implications and management. *J Hepatol* 2003; 39(Suppl. 1): S133–S138.
7 Tipples GA, Ma MM, Fischer KP, Bain VG, Kneteman NM, Tyrrell DL. Mutation in HBV RNA-dependent DNA polymerase confers resistance to lamivudine *in vivo*. *Hepatology* 1996; 24: 714–717.
8 Delaney IV WE, Yang H, Westland CE *et al.* The hepatitis B virus polymerase mutation rtV173L is selected during lamivudine therapy and enhances viral replication in vitro. *J Virol* 2003; 77: 11833–11841.

9 Ono SK, Kato N, Shiratori Y *et al.* The polymerase L528M mutation cooperates with nucleotide binding-site mutations, increasing hepatitis B virus replication and drug resistance. *J Clin Invest* 2001; 107: 449–455.

10 Dienstag JL. Hepatitis B virus infection. *N Engl J Med* 2008; 359: 1486–1500.

11 Angus P, Vaughan R, Xiong S *et al.* Resistance to adefovir dipivoxil therapy associated with the selection of a novel mutation in the HBV polymerase. *Gastroenterology* 2003; 125: 292–297.

12 Villeneuve JP, Durantel D, Durantel S *et al.* Selection of a hepatitis B virus strain resistant to adefovir in a liver transplantation patient. *J Hepatol* 2003; 39: 1085–1089.

13 Fung SK, Andreone P, Han SH *et al.* Adefovir-resistant hepatitis B can be associated with viral rebound and hepatic decompensation. *J Hepatol* 2005; 43: 937–943.

14 Hadziyannis SJ, Tassopoulos NC, Heathcote EJ *et al.* Long-term therapy with adefovir dipivoxil for HBeAg-negative chronic hepatitis B. *N Engl J Med* 2005; 352: 2673–2681.

15 Hadziyannis SJ, Tassopoulos NC, Heathcote EJ *et al.* Long-term therapy with adefovir dipivoxil for HBeAg-negative chronic hepatitis B for up to 5 years. *Gastroenterology* 2006; 131: 1743–1751.

16 Brunelle MN, Jacquard AC, Pichoud C *et al.* Susceptibility to antivirals of a human HBV strain with mutations conferring resistance to both lamivudine and adefovir. *Hepatology* 2005; 41: 1391–1398.

17 Papatheodoridis GV, Manolakopoulos S, Dusheiko G, Archimandritis AJ. Therapeutic strategies in the management of patients with chronic hepatitis B virus infection. *Lancet Infect Dis* 2008; 8: 167–178.

18 Lau DT, Khokhar MF, Doo E *et al.* Long-term therapy of chronic hepatitis B with lamivudine. *Hepatology* 2000; 32: 828–834.

19 Westland CE, Yang H, Delaney IV WE *et al.* Activity of adefovir dipivoxil against all patterns of lamivudine-resistant hepatitis B viruses in patients. *J Viral Hepat* 2005; 12: 67–73.

20 Chang TT, Gish RG, Hadziyannis SJ *et al.* A dose-ranging study of the efficacy and tolerability of entecavir in Lamivudine-refractory chronic hepatitis B patients. *Gastroenterology* 2005; 129: 1198–1209.

21 Tenney DJ, Levine SM, Rose RE *et al.* Clinical emergence of entecavir-resistant hepatitis B virus requires additional substitutions in virus already resistant to Lamivudine. *Antimicrob Agents Chemother* 2004; 48: 3498–3507.

22 Lampertico P, Vigano M, Manenti E, Iavarone M, Sablon E, Colombo M. Low resistance to adefovir combined with lamivudine: a 3-year study of 145 lamivudine-resistant hepatitis B patients. *Gastroenterology* 2007; 133: 1445–1451.

23 Tenney DJ, Rose RE, Baldick CJ *et al.* Long-term monitoring shows hepatitis B virus resistance to entecavir in nucleoside-naive patients is rare through 5 years of therapy. *Hepatology* 2009; 49: 1503–1514.

24 Orito E, Fujiwara K, Tanaka Y *et al.* A case-control study of response to lamivudine therapy for 2 years in Japanese and Chinese patients chronically infected with hepatitis B virus of genotypes Bj, Ba and C. *Hepatol Res* 2006; 35: 127–134.

25 Kobayashi M, Suzuki F, Akuta N *et al.* Response to long-term lamivudine treatment in patients infected with hepatitis B virus genotypes A, B, and C. *J Med Virol* 2006; 78: 1276–1283.

26 Levey AS, Bosch JP, Lewis JB, Greene T, Rogers N, Roth D. A more accurate method to estimate glomerular filtration rate from serum creatinine: a new prediction equation. Modification of Diet in Renal Disease Study Group. *Ann Intern Med* 1999; 130: 461–470.

27 Takahashi M, Nishizawa T, Gotanda Y *et al.* High prevalence of antibodies to hepatitis A and E viruses and viremia of hepatitis B, C, and D viruses among apparently healthy populations in Mongolia. *Clin Diagn Lab Immunol* 2004; 11: 392–398.

28 Inoue J, Ueno Y, Nagasaki F *et al.* Enhanced intracellular retention of a hepatitis B virus strain associated with fulminant hepatitis. *Virology* 2009; 395: 202–209.

29 Tenney DJ, Rose RE, Baldick CJ *et al.* Two-year assessment of entecavir resistance in Lamivudine-refractory hepatitis B virus patients reveals different clinical outcomes depending on the resistance substitutions present. *Antimicrob Agents Chemother* 2007; 51: 902–911.

30 Melegari M, Scaglioni PP, Wands JR. Hepatitis B virus mutants associated with 3TC and famciclovir administration are replication defective. *Hepatology* 1998; 27: 628–633.

31 Peters MG, Hann HW, Martin P *et al.* Adefovir dipivoxil alone or in combination with lamivudine in patients with lamivudine-resistant chronic hepatitis B. *Gastroenterology* 2004; 126: 91–101.

32 Gaia S, Barbon V, Smedile A *et al.* Lamivudine-resistant chronic hepatitis B: an observational study on adefovir in monotherapy or in combination with lamivudine. *J Hepatol* 2008; 48: 540–547.

33 Fung SK, Chae HB, Fontana RJ *et al.* Virologic response and resistance to adefovir in patients with chronic hepatitis B. *J Hepatol* 2006; 44: 283–290.

34 Rapti I, Dimou E, Mitsoula P, Hadziyannis SJ. Adding-on versus switching-to adefovir therapy in lamivudine-resistant HBeAg-negative chronic hepatitis B. *Hepatology* 2007; 45: 307–313.

35 Yatsuji H, Suzuki F, Sezaki H *et al.* Low risk of adefovir resistance in lamivudine-resistant chronic hepatitis B patients treated with adefovir plus lamivudine combination therapy: two-year follow-up. *J Hepatol* 2008; 48: 923–931.

36 Gallego A, Sheldon J, Garcia-Samaniego J *et al.* Evaluation of initial virological response to adefovir and development of adefovir-resistant mutations in patients with chronic hepatitis B. *J Viral Hepat* 2008; 15: 392–398.

37 Chan HL, Wong VW, Tse CH *et al.* Early virological suppression is associated with good maintained response to adefovir dipivoxil in lamivudine resistant chronic hepatitis B. *Aliment Pharmacol Ther* 2007; 25: 891–898.

38 Zollner B, Petersen J, Puchhammer-Stockl E *et al.* Viral features of lamivudine resistant hepatitis B genotypes A and D. *Hepatology* 2004; 39: 42–50.

39 Villet S, Pichoud C, Villeneuve JP, Trepo C, Zoulim F. Selection of a multiple drug-resistant hepatitis B virus strain in a liver-transplanted patient. *Gastroenterology* 2006; 131: 1253–1261.

40 Shaw T, Bartholomeusz A, Locarnini S. HBV drug resistance: mechanisms, detection and interpretation. *J Hepatol* 2006; 44: 593–606.
41 Marcellin P, Chang TT, Lim SG *et al.* Adefovir dipivoxil for the treatment of hepatitis B e antigen-positive chronic hepatitis B. *N Engl J Med* 2003; 348: 808–816.
42 Santantonio T, Fasano M, Durantel S *et al.* Adefovir dipivoxil resistance patterns in patients with lamivudine-resistant chronic hepatitis B. *Antivir Ther* 2009; 14: 557–565.
43 Qi X, Xiong S, Yang H, Miller M, Delaney WE. In vitro susceptibility of adefovir-associated hepatitis B virus polymerase mutations to other antiviral agents. *Antivir Ther* 2007; 12: 355–362.
44 Tan J, Degertekin B, Wong SN, Husain M, Oberhelman K, Lok AS. Tenofovir monotherapy is effective in hepatitis B patients with antiviral treatment failure to adefovir in the absence of adefovir-resistant mutations. *J Hepatol* 2008; 48: 391–398.
45 van Bommel F, Zollner B, Sarrazin C *et al.* Tenofovir for patients with lamivudine-resistant hepatitis B virus (HBV) infection and high HBV DNA level during adefovir therapy. *Hepatology* 2006; 44: 318–325.
46 Choe WH, Kwon SY, Kim BK *et al.* Tenofovir plus lamivudine as rescue therapy for adefovir-resistant chronic hepatitis B in hepatitis B e antigen-positive patients with liver cirrhosis. *Liver Int* 2008; 28: 814–820.
47 Lok AS, McMahon BJ. Chronic hepatitis B. *Hepatology* 2007; 45: 507–539.

SUPPORTING INFORMATION

Additional Supporting Information may be found in the online version of this article:

Table S1 Clonal analysis of HBV RT region of samples from the patient with lamivudine and adefovir resistance.

Please note: Wiley-Blackwell are not responsible for the content or functionality of any supporting materials supplied by the authors. Any queries (other than missing material) should be directed to the corresponding author for the article.

J Gastroenterol (2011) 46:232–241
DOI 10.1007/s00535-010-0297-2

ORIGINAL ARTICLE—LIVER, PANCREAS, AND BILIARY TRACT

Lymphotropic HCV strain can infect human primary naïve $CD4^+$ cells and affect their proliferation and IFN-γ secretion activity

Yasuteru Kondo · Yoshiyuki Ueno · Eiji Kakazu · Koju Kobayashi · Masaaki Shiina · Keiichi Tamai · Keigo Machida · Jun Inoue · Yuta Wakui · Koji Fukushima · Noriyuki Obara · Osamu Kimura · Tooru Shimosegawa

Received: 9 May 2010 / Accepted: 11 July 2010 / Published online: 17 August 2010

Abstract

Background Lymphotropic hepatitis C virus (HCV) infection of B and T cells might play an important role in the pathogenesis of hepatitis C. Recently, we showed that a lymphotropic HCV (SB strain) could infect established T-cell lines and B-cell lines. However, whether HCV replication interferes with cell proliferation and function in primary T lymphocytes is still unclear.

Aim The aim of this study was to analyze whether HCV replication in primary T lymphocytes affected their development, proliferation, and Th1 commitment.

Methods SB strain cell culture supernatant (2×10^4 copies/ml HCV) was used to infect several kinds of primary lymphocyte subsets. Mock, UV-irradiated SB-HCV, JFH-1 strain, and JFH-1 NS5B mutant, which could not replicate in T cells, were included as negative controls. Carboxyfluorescein succinimidyl ester (CFSE) and CD45RA double staining was used to evaluate the proliferative activity of $CD4^+CD45RA^+CD45RO^-$ naïve $CD4^+$ cells. Interferon (IFN)-γ and interleukin (IL)-10 secretion assays magnetic cell sorting (MACS) were carried out.

Results Negative strand HCV RNA was detected in $CD4^+$, $CD14^+$, and $CD19^+$ cells. Among $CD4^+$ cells, $CD4^+CD45RA^+RO^-$ cells (naïve $CD4^+$ cells) were most susceptible to replication of the SB strain. The levels of CFSE and CD45RA expression gradually declined during cell division in uninfected cells, while HCV-infected naïve $CD4^+$ cells expressed higher levels of CFSE and CD45RA than Mock or UV-SB infected naïve $CD4^+$ cells. Moreover, the production of IFN-γ was significantly suppressed in SB-infected naïve $CD4^+$ cells.

Conclusions Lymphotropic HCV replication suppressed proliferation and development, including that towards Th1 commitment, in human primary naïve $CD4^+$ cells.

Keywords HCV · Lymphotropic · Naïve $CD4^+$ cell · Th1

Electronic supplementary material The online version of this article (doi:10.1007/s00535-010-0297-2) contains supplementary material, which is available to authorized users.

Y. Kondo · Y. Ueno (✉) · E. Kakazu · M. Shiina · K. Tamai · J. Inoue · Y. Wakui · K. Fukushima · N. Obara · O. Kimura · T. Shimosegawa
Division of Gastroenterology,
Tohoku University Graduate School of Medicine,
1-1 Seiryo, Aobaku, Sendai 980-8574, Japan
e-mail: yueno@med.tohoku.ac.jp

K. Machida
Department of Molecular Microbiology and Immunology,
University of Southern California Keck School of Medicine,
2011 Zonal Avenue, Los Angeles, CA 90033, USA

K. Kobayashi
School of Health Science, Tohoku University, 1-1 Seiryo,
Aobaku, Sendai 980-8574, Japan

Introduction

Hepatitis C virus (HCV) infects about 170 million people worldwide and is a major cause of chronic hepatitis, liver cirrhosis, and hepatocellular carcinoma (HCC) [1]. Cellular and humoral immune responses to HCV play an important role in the pathogenesis of chronic hepatitis, liver cirrhosis, HCC, and B-lymphocyte proliferative disorders, including mixed cryoglobulinemia, a disorder characterized by the oligoclonal proliferation of B cells [2, 3].

Several mechanisms have been proposed for the failure of the cellular immune response, including anergy, cytotoxic T-lymphocyte (CTL) exhaustion, suppression via

regulatory $CD4^+$–$CD25^+$ T cells interleukin-10 (IL-10)-secreting regulatory $CD8^+$-T cells, and direct binding of HCV core antigen [4–7]. However, the influence of HCV replication in lymphoid cells on their functions is not fully understood. HCV replicates primarily in the liver, but HCV-RNA has been detected in other lymphoid cells, including B- and T-lymphocytes, monocytes, and dendritic cells [8–11]. Sung et al. [12] have previously reported a B-cell line (SB cells) that produces HCV particles that can further infect B lymphocytes in vitro. We have shown that the SB-HCV strain could infect and replicate in T-cell lines and that HCV replication could inhibit interferon (IFN)-γ/signal transducer and activator of transcription-1 (STAT-1)/T-bet signaling of the T cells [13]. Moreover, we reported that HCV replication in Molt-4 could affect the proliferation and FAS-mediated apoptosis of T cells by inhibiting CD44v6 expression and mitogen-activated protein kinase (MAPK) signaling in Molt-4 [14]. Most of these data came from studies using cell lines, since stable SB-HCV replication could be detected in lymphoid cell lines (Raji, Molt-4, etc.). However, the analysis of primary lymphocytes is preferable to determine the real effects of lymphotropic HCV strains on T-cell biology. In fact, the effects of low titers of HCV in primary T cells have not been clarified yet.

We first reported that, among T cells, $CD4^+CD45RA^+RO^-$ naïve T cells were susceptible to SB-HCV infection [13]. Here we describe the functional and proliferative analysis of SB-HCV-infected naïve $CD4^+$ T cells after short-term culture.

Materials and methods

Culture of cell lines

SB cells that continuously produce infectious HCV particles were originally established from splenocytes of an HCV-infected patient with type 2 mixed cryoglobulinemia and monocytoid B-cell lymphoma [12]. The cells were maintained in standard RPMI (Invitrogen, Carlsbad, CA, USA) medium with 20% fetal bovine serum (FBS) without any supplement. Every 5 days, the cells were sedimented by natural gravity for 30 min at 37°C.

In vitro infection of primary lymphoid cells

Supernatants from SB cells were purified by centrifugation and 0.2-μm filter. SB culture supernatant (5 ml), which contained 2.2×10^4 copies/ml of HCV RNA, was used for the infection of several kinds of human primary lymphoid cells (1×10^5 cells). A control infection with UV-irradiated SB culture supernatant was included in every experiment. Supernatants of Huh7.5 cells transfected with JFH-1 strains [15–17] at 10 days post-transfection were used for several control experiments. Cells were washed 3 times at 2 days after infection. Then, a portion of the cells (3×10^5 to 5×10^5 cells) was harvested for analysis; the remaining cells (1×10^5 cells) were kept and incubated under the same condition.

Isolation of various kinds of lymphoid cells and naïve $CD4^+$ T cells

We got informed consent from 5 healthy donors, from whom peripheral blood mononuclear cells (PBMC) were isolated by Ficoll-Paque centrifugation (Amersham Bioscience [Uppsala, Sweden]). Anti-CD3 phycoerythrin (PE), anti-CD4 (PE-Cy3), anti-CD8 (PE), anti-CD14 (PE), anti-CD19 (PE), anti-CD45RO (PE), and antiCD45RA (fluorescein isothiocyanate [FITC]) antibodies (BD Pharmingen) were used for the separation of different kinds of mononuclear cells by using fluorescence activated cell sorting (FACS) vantage (BD Parmingen, San Jose, CA, USA). In some experiments, a naïve $CD4^+$ T cell isolation kit II (Miltenyi Biotec [Bergish Gladbach, Germany]) was used to obtain more viable naïve $CD4^+$ cells.

Strand-specific intracellular HCV RNA detection

Strand-specific intracellular HCV RNA was detected by using a recently established procedure that combined previously published methods [9, 18] with minor modifications [13]. Positive- and negative-strand-specific HCV RNAs were detected by a nested polymerase chain reaction (PCR) method. Reactions were performed with 2 μl of 10× reverse transcriptase (RT) buffer, 2 μl of 10-mmol/l magnesium chloride, 200-μmol/l each of deoxyadenosine triphosphate, deoxycytidine triphosphate, deoxyguanosine triphosphate, 100-μmol/l of thymidine triphosphate (dTTP), 0.2 U of uracil-*N* glycosylase (UNG; Perkin Elmer [Fremount, CA, USA]/Applied Biosystems), 5 U of rTth DNA Polymerase; and 50 pmol of strand-specific HCV primers (positions according to the 5′ untranslated region), nt −285 to −256 (ACTGTCTTCACGCAGAAAGCGTCT AGCCAT) and −43 to −14 (CGAGACCTCCCGGGGCA CTCGCAAGCACCC) and template RNA. The RT mixture was incubated for 10 min at room temperature and then at 70°C for an additional 15 min. The cDNA product was subjected to the first PCR with 80 μl of PCR reaction buffer containing 50 pmol of HCV downstream strand-specific primer. The PCR amplification consisted of 5 min at 95°C, followed by 35 cycles (1 min at 94°C, followed by 1 min at 67°C, and then by 1 min at 72°C), and then 7-min extension at 72°C. For the second nested PCR, an aliquot (1/10) of the first PCR reaction mixture was re-amplified

using 50 pmol of each of the two primers, nt −276 to −247 (ACGCAGAAAGCGTCTAGCCATGGCGTTAGT) and nt −21 to −50 (TCCCGGGGCACTCGCAAGCACCCT ATCAGG), which span the 255-base pair region nt −276 to −21 (position according to the 5′ untranslated region) of HCV RNA, and Taq polymerase (Applied Biosystems). The reaction was run for 35 cycles (1 min at 94°C, 1 min at 67°C, 1 min at 72°C), followed by 7 min at 72°C. Semi-quantification was achieved by serial fourfold dilutions (in 10 μg/ml of *Escherichia coli* tRNA) of an initial amount of 200 ng of total RNA. The relative titer was expressed as the highest dilution giving a visible band of the appropriate size on a 2% agarose gel stained by ethidium bromide. For internal control, semi-quantification of β-actin mRNA was performed by using the same RNA extracts. To rule out false, random, and self-priming, extracted HCV RNA was run in every RT–PCR test without the addition of an upstream HCV primer.

CFSE staining

Cells were analyzed by using a CellTrace CFSE Cell Proliferation Kit (Invitrogen [Carlsbad, CA, USA]). The cell staining methods followed the manufacturer's protocol. Stained cells were washed three times and incubated for an additional 7 days. Cells were analyzed by flow cytometry with 510 nm excitation and emission filters. A proliferation index was calculated by FlowJo 7.5 (Tree Str Inc, Ashland, OR, USA), according to the manufacturer's protocol.

Annexin V and propidium iodide staining

Cells were stained with Annexin V and propidium iodide (PI) by using an apoptosis detection kit (R&D systems, Minneapolis, MN, USA). Staining methods were conducted according to the manufacturer's protocol. Briefly, collected cells were washed and gently re-suspended in the Annexin V incubation reagent at a concentration of 3×10^5 cells per 100 μl. Then, re-suspended cells in binding buffer were stained by Streptavidin conjugate allophycocyanin (APC) and analyzed by flow cytometry within 1 h.

Transfection of HCV individual protein expression plasmids

The various expression plasmids were constructed by inserting HCV core, E1, E2, NS3, NS4B, NS5A, and NS5B cDNA of genotype 1a [19] behind the cytomegalovirus virus immediate-early promoter in pCDNA3.1 (Invitrogen). Primary $CD4^+$ cells were transfected using Nucleofector I (Amaxa, Gaithersburg, Washington DC, USA) with a Human T cell Nucleofector kit (Amaxa), and various plasmids were purified using the EndFree plasmid kit (QIAGEN, Valencia, CA, USA). Viable transfected cells were isolated by Ficoll-Paque centrifugation (Amersham Bioscience) at 24 h post-transfection. Transfection and expression efficiency were analyzed by using intracellular staining of HCV individual proteins and flow cytometry analysis. Briefly, the cells were fixed and permeabilized with fixation/permeabilization solution (BD Bioscience) at 4°C for 25 min. The cells were then washed two times in BD Perm/Wash buffer (BD Bioscience) and resuspended in 50 μl of BD Perm/Wash buffer containing pre-conjugating polyclonal anti-E1, E2, NS3, NS4B, NS5B, NS5A antibody (abcam, Cambridge, MA, USA) with a phycoerythrin (PE)-conjugated anti-mouse antibody.

Confocal laser microscopy

Primary lymphocytes (3×10^6 cells/ml) in suspension were fixed and permeabilized with fixation/permeabilization solution (BD Bioscience) at 4°C for 25 min. The cells were then washed two times in BD Perm/Wash buffer (BD Bioscience) and resuspended in 50 μl of BD Perm/Wash buffer containing pre-conjugating polyclonal anti-NS5A antibody (Biodesign International, Saco, ME, USA) with an FITC-conjugated anti-mouse antibody.

Interferon-γ and interleukin 10 secretion assay

Cells were washed by adding 2 ml of cold phosphate-buffered saline (PBS) and resuspended in 90 μl of cold RPMI 1640 medium. After the addition of 10 μl of IL-10- or IFN-γ-Catch Reagent (Miltenyi Biotec), cells were incubated for 5 min on ice. Then the cells were diluted with 1 ml of warm medium (37°C) and further incubated in a closed tube for 45 min at 37°C under slow continuous rotation. Cells were washed and IL-10- or IFN-γ-secreting cells were stained by adding 10 μL of IL-10- or IFN-γ-detection antibody (PE-conjugated) (Miltenyi Biotec) together with anti-CD4-PerCP.

Real-time PCR analysis

Cells were collected sequentially at various time points after the addition of recombinant human IFN-γ (500 ng/ml) (BD Biosciences, CA, USA). After the extraction of total RNA and the RT procedure, real-time PCR using a TaqMan Chemistry System was carried out. The ready-made set of primers and probe for the amplification of T-bet (ID HS00203436) and glyceraldehyde-3-phosphate-dehydrogenase (GAPDH) were purchased from Perkin-Elmer/Applied Biosystems. The relative amount of target mRNA was obtained by using a comparative the threshold cycle (CT) method. The expression level of mRNAs of the non-stimulation sample of vector transfected-primary

$CD4^+$ cells was represented as 1.0 and the relative amount of target mRNA in a stimulated sample was calculated according to the manufacturer's protocol.

Immunoblot assay

Proteins were resolved by electrophoresis in sodium dodecyl sulfate–polyacrylamide gels and electrophoretically transferred onto a polyvinylidene difluoride (PVDF) membrane (Bio-Rad, Hercules, CA, USA). The membrane was incubated with anti-STAT-1α, or anti-p-STAT-1 antibodies (Cell Signaling, Danver, MA, USA) and then reacted with peroxidase-conjugated secondary antibody. Immunoreactivity was visualized by an enhanced chemiluminescence detection system (Amersham Bioscience).

Statistical analysis

Statistical analyses of the data in Figs. 1c, 2c, 3b, and 4 were performed by the analysis of variance (ANOVA)

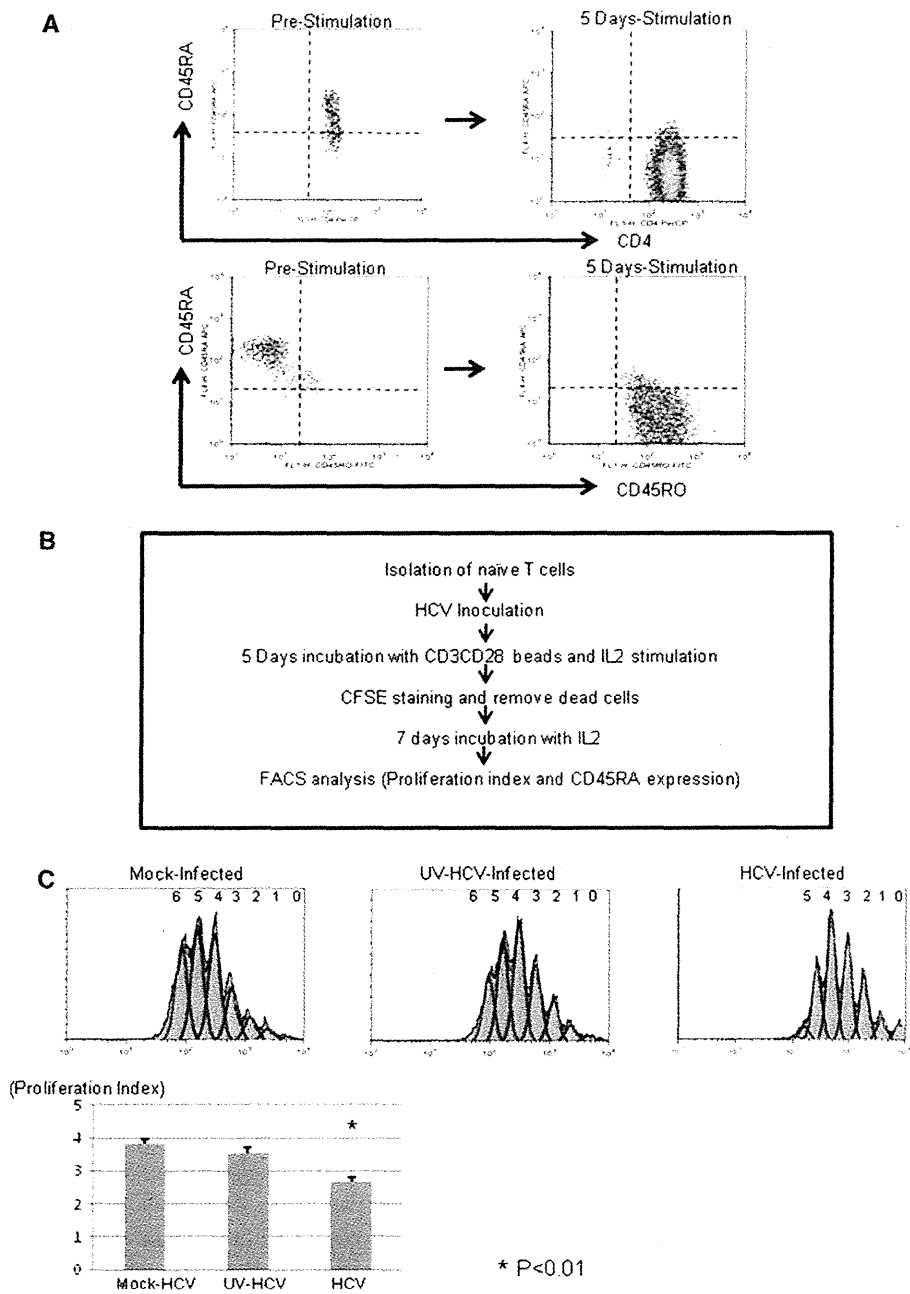

Fig. 1 Suppression of proliferation activity in hepatitis C virus (*HCV*)-infected human naïve T lymphocytes. **a** A representative dot plot of $CD4^+CD45RA^+RO^-$ cells is shown. Cells are stained with CD4-PerCP-antibody (Ab), CD45RA-fluorescein isothiocyanate (FITC)-Ab, and CD45RO-APC-Ab. The purity of isolated $CD4^+CD45RA^+RO^-$ naïve T lymphocytes is over 92%. **b**, **c** Carboxyfluorescein succinimidyl ester (CFSE) staining was carried out at 5 days post-infection in SB-HCV, UV-irradiated HCV, and Mock. Stained cells were washed three times and incubated for an additional 7 days with T-cell expander. Cells were analyzed by flow cytometry with 510 nm excitation and emission filters. *Numbers* in the representative histogram indicate numbers of cell divisions. The proliferation index was calculated by FlowJo 7.5 software according to the manufacturer's protocol. The proliferation index is shown in this *bar graph*. Three independent experiments were carried out. *Error bars* indicate the standard deviation. *IL* interleukin

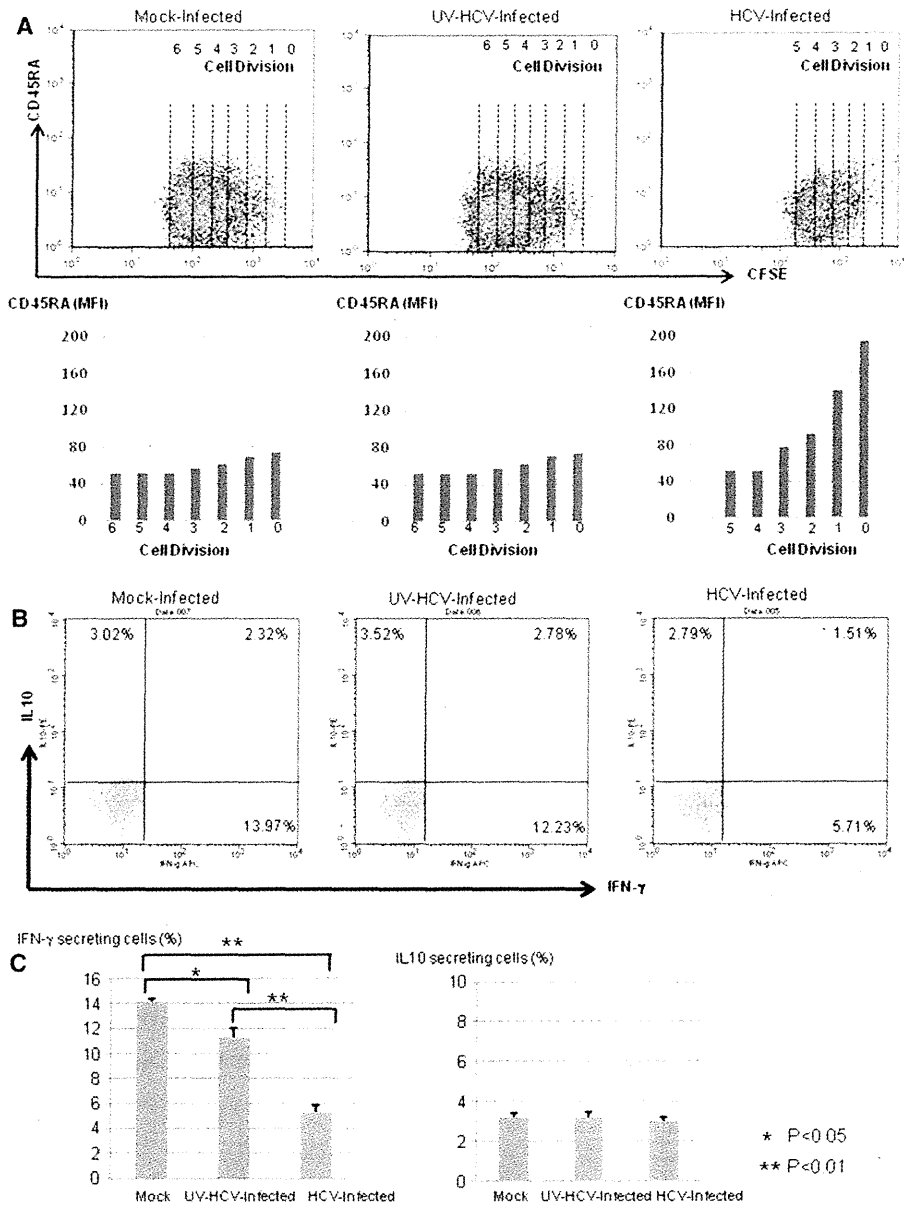

Fig. 2 Suppression of development and Th1 commitment in HCV-infected human naïve T lymphocytes. **a** Representative dot plots of CD45RA and carboxyfluorescein succinimidyl ester (CFSE) double staining are shown. *Numbers* in the representative dot plots indicate the numbers of cell divisions. *Bar graphs* indicate the mean fluorescence intensity (MFI) of cell clusters. **b** Representative dot plots of interferon-γ (*IFN-γ*) and interleukin (IL) 10 secretion assays are shown. The *numbers* in the quadrant indicate IFN-γ and/or IL10-secreting cells among $CD4^+$ cells. **c** The frequencies of IFN-γ- and IL10-secreting cells among the three groups are shown in these *bar graphs*. Three independent experiments were carried out. *Error bars* indicate the standard deviation

test (SPSS10.0, SPSS Inc, Chicago, IL, USA). Values of $p < 0.05$ were considered to be statistically significant.

Results

Detection of negative-strand HCV-RNA among lymphoid cells

Strand-specific rTth based nested PCR was carried out to analyze the susceptibility to HCV infection among the various kinds of lymphoid cells with or without short term culture (7 days). Isolated lymphoid cells were infected with SB-HCV, UV-irradiated-HCV, or JFH-1 strain and were cultured with appropriate cytokines and/or antibody stimulation (Table 1). We needed to add different kinds of cytokines to maintain the cell proliferation and viability. Negative-strand HCV-RNA could be detected in $CD4^+$, $CD14^+$, and $CD19^+$ cells and in $CD8^+$ cell-depleted PBMCs (PBMC-$CD8^+$) after short-term culture (Table 2). However, negative- and positive-strand HCV-RNA could not be detected in any kinds of lymphoid cells infected with the supernatant of JFH-1 and JFH-1 GND mutant (data not shown). Undetectable negative-strand HCV-RNA at 2 days post-infection indicated that HCV-RNA was replicated after inoculation. We found that depletion of $CD8^+$ cells from

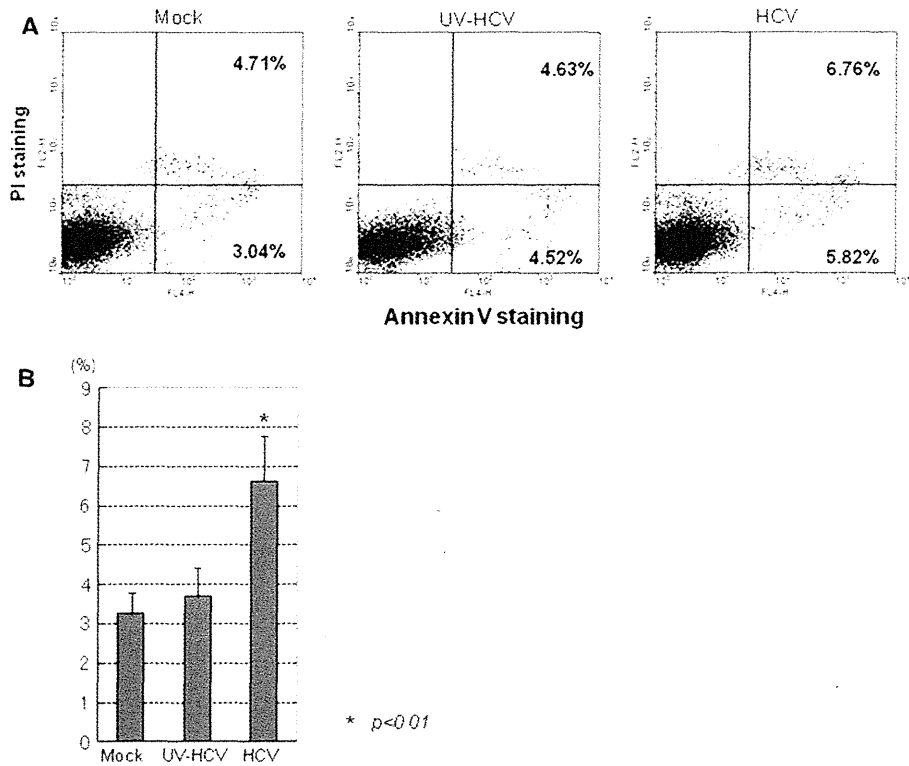

Fig. 3 HCV replication induces apoptosis of naive $CD4^+$ cells. **a** Representative dot plots of Annexin V and propidium iodide (*PI*) staining are shown. The *numbers* in the quadrants indicate the frequencies of early apoptotic cells (Annexin V^+ and PI^-) and dead cells (Annexin V^+ and PI^+ cells). **b** The frequencies of early apoptotic cells are shown in this *bar graph*. Three independent experiments were carried out. *Error bars* indicate the standard deviations

PBMCs was favorable to replication in lymphoid cells. In this study, we used CD3CD28 beads and IL2 stimulation that could stimulate more efficiently than CD3 and IL2 stimulation. However, among the $CD4^+$ cells, $CD4^+$ $CD45RA^+RO^-$ naïve $CD4^+$ cells were most susceptible to infection, as we previously demonstrated (Table 2) (Suppl. Fig. 1) [13]. These data indicate that $CD4^+CD45RA^+RO^-$ naïve $CD4^+$ cells could be infected with SB-HCV during T-cell development. CD81 was one of the main candidates of HCV receptors for the infection of the cells [20–22]. We tried to analyze whether anti-CD81 antibody might block the SB-HCV infection of primarily naïve $CD4^+$ cells. HCV-NS5A protein could be detected in 12.2% of SB-HCV-inoculated naïve $CD4^+$ cells at 10 days post-infection. However, the pretreatment of anti-CD81 antibody reduced the frequency of NS5A detection among the SB-HCV-inoculated naïve $CD4^+$ cells (4.7%) (Suppl. Fig. 2). The sensitivity of NS5A immunostaining was lower than that of the strand-specific nested PCR method [13].

Suppression of proliferation activity in SB-HCV-infected naïve $CD4^+$ cells

The purity of $CD45RA^+RO^-$ naïve $CD4^+$ cells after isolation was around 92% (Fig. 1a). CFSE staining was carried out at 5 days post-infection in SB-HCV, UV-irradiated HCV, and Mock. Stained cells were washed three times and incubated for an additional 7 days with T-cell expander (CD3CD28 coated beads and IL2 stimulation). Cells were analyzed by flow cytometry with 510 nm excitation and emission filters. The proliferation index was calculated by FlowJo 7.5 software according to the manufacturer's protocol. The proliferation index of SB-HCV-infected naïve $CD4^+$ cells was significantly lower than that of controls ($p < 0.01$) (Fig. 1b, c). These data indicate that lymphotropic SB-HCV suppresses the proliferation activity of T cells.

Disturbance of cell development and IFN-γ-secreting activity

CD45RA and CFSE double staining was carried out to analyze the cell development. The expression level of CD45RA on naïve $CD4^+$ cells had gradually declined during cell proliferation. However, the CD45RA expression level of SB-HCV-infected naïve $CD4^+$ cells remained higher than those of the control groups (Fig. 2a). Moreover, the frequency of IFN-γ-secreting cells among SB-HCV-infected $CD4^+$ cells was significantly lower than those of the control groups ($p < 0.01$) (Fig. 2b, c). On the other hand, the frequency of IL10-secreting cells was comparable in the three groups (Fig. 2b, c). These data indicate that HCV infection could interrupt cell development, especially Th1 development.